A Pulsed Eddy Current System for Flaw Detection Using an Encircling Coil on a Steel Pipe

Shiva Majidnia[*1, 2], John Rudlin[2], Rajagopal Nilavalan[1]

[1]Brunel University, Uxbridge, United Kingdom

[2]TWI Ltd, Cambridge, United Kingdom

shiva.majidnia@brunel.ac.uk

Abstract

Conventional eddy current techniques have been used to a great extent for detection of surface breaking defects in conductive materials. However, detection of sub-surface defects is limited due to skin effect phenomena and material properties. Pulsed Eddy Current (PEC) techniques excite the probe's driving coil with a repetitive broadband pulse, usually a square wave. The resulting transient current through the coil induces transient eddy currents in the test piece, these pulses consist of a broad frequency spectrum, and the reflected signal contains important depth information.

The work in this paper employs COMSOL Multiphysics, the finite element (FE) modelling software, to investigate the behaviour of a new encircling probe design. This work involves modelling of an encircling coil around a steel pipe with high lift-off to simulate insulation. The 3D modelling of the coil wrapped around a steel pipe was employed and surface breaking discontinuities were modelled. The simulation of these scenarios provided essential information about the behaviour of this probe design.

Key words: Pulsed Eddy Current, Non-Destructive Testing, Defect Detection, Finite Element Method, Encircling Coil, Corrosion under insulation

1. Introduction

Corrosion under insulation of process pipework is a serious problem for oil and gas industries, and is difficult to detect because of the insulation cover that masks the corrosion problem until it is too late. This type of corrosion can cause failures in not inspected and treated. The most effective method is to remove the insulation, inspect the surface condition of the pipe and replace the insulation. However this method is very time consuming and costly and may also cause problems while the pipe is in service [1].

Pulsed Eddy Current has been used to approach this problem [2,3] but the method is slow because of use of pancake coils. In order to increase the scanned area, an encircling coil has been proposed, with a view to inspect a complete circumference with a single pulse. The work presented here is a part of the development of the equipment.

1.1. Principle of Eddy Current Technique

Eddy current techniques use a coil for field excitation, and eddy currents are induced within the conductors and flow in opposite direction to the exciting currents. The induced eddy currents are associated with highly attenuated magnetic pulses propagating into the material [2]. The schematic diagram of eddy current technique is illustrated in Figure 1.

In traditional Eddy Current techniques, a sinusoidal AC current is used to excite the coil. Whereas in PEC, the probe's driving coil is excited with a repetitive broadband pulse, usually a square wave. Since the produced pulses consist of a broad frequency spectrum, the reflected signal

contains important depth information [3]. Physically, the pulse is broadened and delayed as it travels deeper into the highly dispersive material, and flaws or other anomalies close to the surface affect the Eddy current response earlier than deeper flaws. Peak values and peak times have been used for flaw detection and identification. [4]

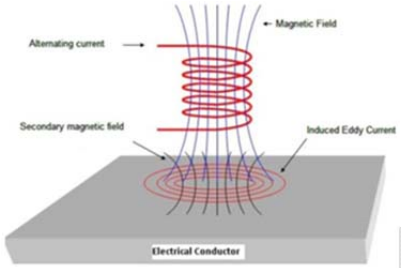

Figure 1. Eddy Current Generation [5]

2. Driver Coil Parameters

In order to find out the optimum number of turns for the given driver circuit, inductance of the coil for different number of turns was calculated. Equation below shows the general formula for inductance calculation [6]:

$L = \frac{N^2 \mu_0 \mu_r A}{l}$	(1)

Where **L** is inductance of the coil in Henries(H), l is the lenght of the coil in meters (m), μ_0 is the permeability of free space ($4\Pi \times 10^{-7}$), μ_r is the reletive permeability of the core material, **N** is the number of turns and **A** is area of cross-section of the coil in square metres (m^2). In Table 1, r_1 and r_2, are radius of the inside and outside of the coil in meters respectively. CA is Maximum current amplitude in Ampers and MF is the maximum magnetic field in Oersted at the appointed point at the center of the coil.

Table 1 Description of Design Parameters for Driver Coil

	N=10			N=20		
	1 layer	2 layers	Coil with longitudinal spacing	1 layer	2 layers	Coil with longitudinal spacing
L(uH)	71.1	78.8	58	227.5	276.7	162.5
N	10	10	10	20	20	20
r_1	0.18	0.18	0.18	0.18	0.18	0.18
r_2	0.18	0.184	0.18	0.18	0.184	0.18
l	0.04	0.02	0.076	0.08	0.04	0.16
CA(A)	28	25	32	12	10	15
MF (Oe)	41	51	28	22.5	28.4	17

Having carried out studies above and finding the maximum magnetic field, a 10 turn coil with 2 layers was chosen to be used.

3. Eddy Current Modelling Using COMSOL Multiphysics

In order to model the behaviour of an eddy current system as applied for non-destructive testing, the magnetic field interface of AC/DC module of COMSOL Multiphysics was used. The magnetic fields interface has the equations and external currents for modelling magnetic fields and solving for the magnetic vector potential [7]. The main feature is the Ampère's Law feature, which adds the equation for the magnetic vector potential and provides an interface for defining the constitutive relation and its associated properties such as the relative permeability.
The notations used in the following equations are defined in Table 2.
The transient magnetic fields are computed by solving for equations below:

$\sigma \frac{\partial A}{\partial t} + \nabla \times H = J$	(2)
$B = \nabla \times A$	(3)
$B = \mu H$	(4)

To obtain a closed system, the constitutive relationships describing the macroscopic properties of the medium are also needed, as described below:

$D = \varepsilon_0 E + P$	(5)
$B = \mu_0 (H + M)$	(6)
$J = \sigma E$	(7)

The electric polarization vector, **P**, is generally a function of **E** and describes how a material is polarized when an electric field, **E**, is present. Some materials can have a non-zero **P** in the absence of an electric field.
The magnetization vector, **M**, is a function of **H**, and similarly describes how a material is magnetized when a magnetic field, **H**, is present. One use of the magnetization vector is to describe permanent magnets, which have a non-zero **M** when no magnetic field is present.
For linear materials, the polarization is directly proportional to the electric field and magnetization is directly proportional to the magnetic field. In this paper, all the materials are considered to be in their linear ranges.
To get a full description of an electromagnetics problem, boundary conditions must be specified at physical boundaries where the magnetic potential is set to 0. The air domain boundaries are specified here as the magnetic insulation boundaries [8].

Table 2 Notation Used in the Equations

Symbol	Quantity	Symbol	Quantity
E	Electric field intensity	**M**	Magnetization vector
H	Magnetic field intensity	**A**	Magnetic vector potential
D	Electric flux density	μ	Magnetic permeability
B	Magnetic flux density	σ	Electric conductivity
J	Current density		

3.1. The Model

When modelling a multi-turn coil, it is not necessary to model the connecting leads and individual wires. The software models a homogenized current carrying region to compute the magnitude and direction of the current flow. It then uses this information to find the magnetic field in and around

the conductor. An air domain is created around the coil and tube to realistically model the magnetic flux path. The boundaries of this air domain are magnetically insulated which ensures that flux does not diverge out of the modelling domain [9].
A 50 mm gap was modelled to simulate a non- conductive insulation. The tube was modelled with a wall thickness of 10mm, the length of the tube was considered to be long enough for the model; however it was not as long as the tube used in experiments, to avoid unnecessary mesh elements in the model [10]. A steel pipe was used in the model with relative magnetic permeability of 1000 (material is considered to be in linear magnetization range at the stage of this work) and electrical conductivity of 1.25 MS/m.
Figure 2(a) shows the voltage input to the driver and Figure 2(b) illustrates current at the coil. These signals were captured using LT spice software which was used to simulate the driver circuit. The current used to excite the coil in simulation is created using a piecewise function and is shown in Figure 3.

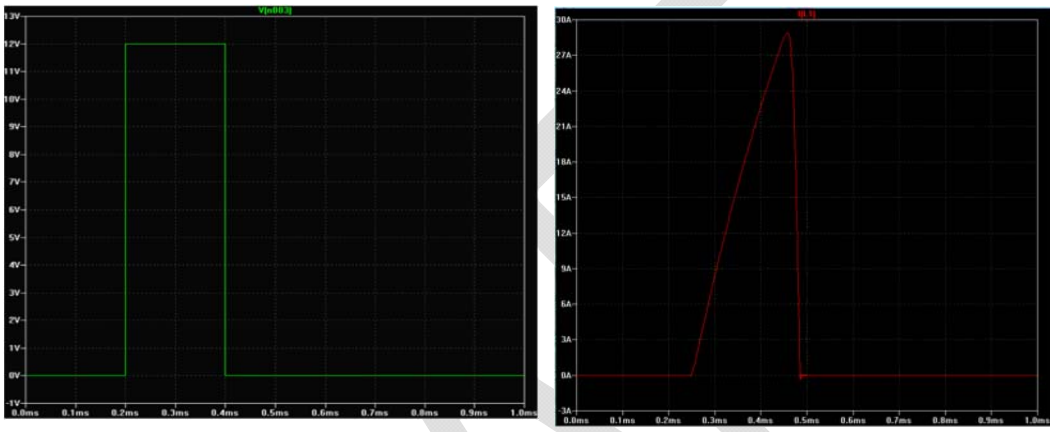

Figure 2.(a) Input voltage to the driver circuit (b) Current at the coil

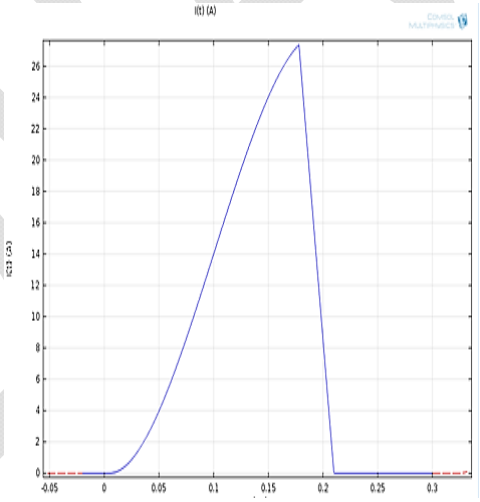

Figure 3. Current Used to Drive the Coil in Simulation

A series of simulations were carried out to find the best place for the magnetic field sensors. This was done by using the difference in the magnetic field a coil in the air and a coil around the tube [3].
Table 3 indicates the positions used. These sensors can also be schematically observed in Figure 4.

Table 3 Position of Sensors

position	Description
1	Center, inside of the coil former
2	Center, outside of the coil former
3	Tube surface ,center of the coil former
4	25 mm below center of the coil former
5	25 mm above the center of the coil former
6	25 mm to the side of coil former
7	25 mm below and 25 mm to the side

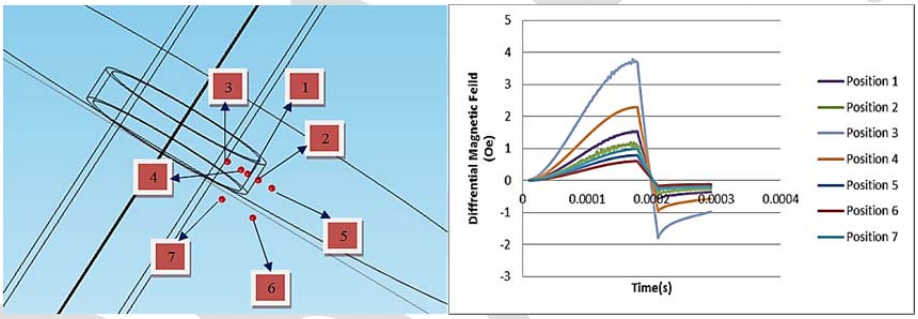

Figure 4. (a) Schematics of Sensor Positions (b) Differential Magnetic Field

The results from the graph in Figure 4 are the differential signals which are calculated by subtracting the reference signal from test signal. The reference signal is the signal from coil in air and the test signal is coil around the pipe. The biggest signal is received at position 3.This position however is not accessible due to the presence of insulation. Position 4 is the second best position between the ones illustrated in this section but again would not be useable due to the same problem. As a result position 1 was chosen to be used at this stage.

4. Coil Shielding

It is believed that shielding an eddy current coil with a material with high permeability concentrates the magnetic field and reduces the lateral spread (Surface coils) [5]. This was investigated in this encircling coil arrangement using the modelling software. A layer of steel with relative permeability of 240 and conductivity of 1.25×10^6 (S/m) was covering the coil with a 10 mm gap in the 3D model, (Ferrite cores used for the core and shielding have a lot lower conductivity and higher permeability).Steel strip was used at this stage due to accessibility. The results shown in this paper are in accordance to the ones stated in Table 3. Figure 5(a) shows a 2D cross section of the coil around the tube and Figure 5(b) shows the coil around the tube with steel shielding. As can be observed the magnetic field at the position of the coil reduces as the steel strip

provides a new path for the magnetic field to flow. Figure 6 shows the difference between the magnetic field at positions shown in grey in Table 3 with and without shield.

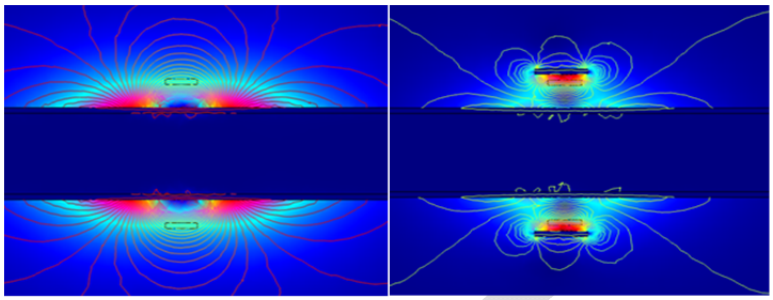

Figure 5 (a) Coil With-Out Shielding (b) Coil with Steel Shielding

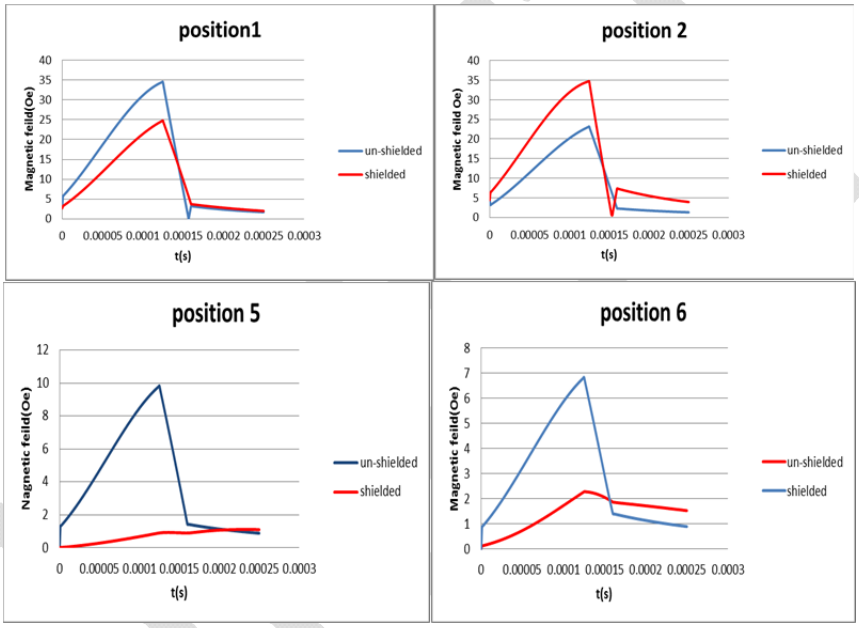

Figure 6. Magnetic Fields at Each Position With and With-Out Shielding

It is evident from the results that in this case of encircling coil, shielding with the steel strip is not proving a benefit. Although it did not help the situation it was decided to further investigate to find out whether the introduction of a flaw will make a noticeable distortion to the magnetic field at each sensor. This was done by introducing a fairly deep corrosion type flaw with 80% of wall thickness depth. The difference between the magnetic fields is obtained from subtracting the flaw signal from the reference signal [11]. (Reference signal was the magnetic field at the position of sensor when there was no flaw in the material) the discrepancy of the magnetic fields at each position is calculated and can be found in graphs of Figure 7.

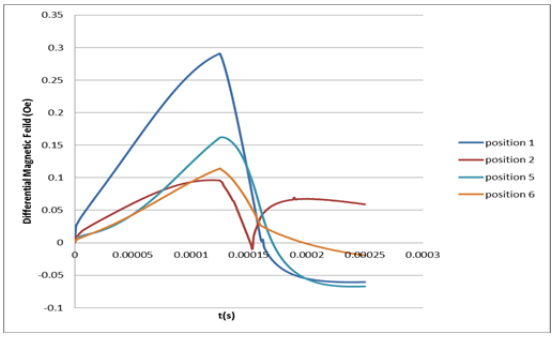

Figure 7. Differential Magnetic Field with Shielded Coil

The greatest difference at sensor 1 is about 0.28 Oe (1 Oe is 1 Gauss in air). The same size flaw in section 6 from an unshielded coil gave a difference of about 1.3 Oe. This confirms that shielding of the coil is not beneficial.
In the next section discontinuities were introduced to the pipe and the magnetic field was captured at each point.

5. Surface Flaws

In this section surface discontinuities were introduced to the pipe and the magnetic field was captured at the appointed position. The discontinuities were surface breaking corrosion type flaws which had depths varying from 10, 20, 40,80and 100% of wall thickness. The width was 25 mm and the length was 55 mm. These dimensions were kept constant.
The results can be found in Figure 8. Information extracted from this graph can then be used in choosing an appropriate magnetic field sensor. Simulation results suggest that a chosen sensor should have a saturation field greater than 35 Oe. The sensitivity range of a sensor should also be considered, meaning a sensor needs to be sensitive to variations as small as 0.5 Oe and lower to detect smaller flaws.
This should be noted that these results are from an ideal situation (modelling).

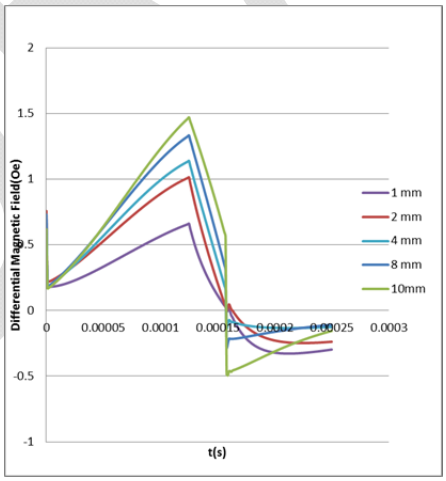

Figure 8. Differential Magnetic Field at the Appointed Sensor Position

Figure 8 demonstrates that the depth of surface flaws have a significant effect on the peak value of the response signals.

6. Overall System Description

For testing purposes a pulsed eddy current experimental platform was built to obtain testing signals. The experimental set-up consisted of a waveform generator, a driver coil, magnetic field sensors, A/D card and a PC with signal processing software installed on it.
The waveform generator feeds the rectangular signal to the driver circuit which excites the driver coil. The pick-up devices measure the magnetic field which then is amplified and fed to the A/D card. The digitized data will be used for feature extraction and result interpretation. Finally the results will be displayed on the monitor for interpretation by the user. The diagram of such a system is illustrated below in Figure 9.

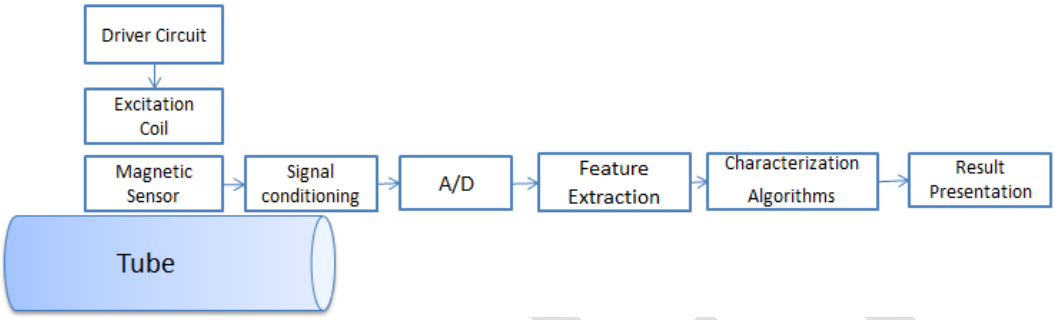

Figure 9 PEC Experimental System's Description

7. Some Practical Results

In this section a typical time response of the proposed system is shown. A magnetometer was chosen for these experiments with an excellent sensitivity to applied magnetic field. This magnetic field sensor produces a voltage proportional to the magnetic field applied to it. The results in Figure 10 are showing the capability of this system. Comparison of results is out of the scope of this paper and will be published separately.

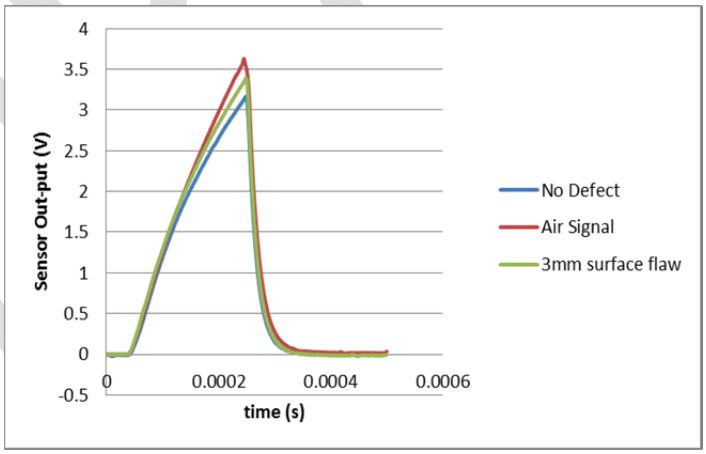

Figure 10.PEC Sensor Response

8. Conclusion

This work explored a Pulsed Eddy Current system behaviour using finite element software which involved an encircling coil around a steel pipe with non-conductive insulation and magnetic field sensors. The system appeared to be able to detect surface corrosion type flaws in steel pipe. FEA proved to be a useful tool to identify the appropriate sensors and their locations.

9. Future Work

In the next stage of this work, detection of flaws under a metal cover (galvanized steel cover over insulation) will be studied. To do this it will be necessary to extend the modelling to the non-linear range of magnetic properties of the material. Shielding of the coil using a material with higher permeability and lower conductivity will be investigated. A multi-channel system will also be built to conduct a complete circumference inspection.

10. References

[1] M. Twomey, "Inspection Techbiques For Detecting Corrosion Under Insulation," Gregory C. Alvarado, 1998.

[2] J. G. Martin, J. G. Gil and E. V. Sánchez, "Non-Destructive Techniques Based on Eddy Current Testing," Sensors-Open access, vol. 11, pp. 2526-2565, 2011.

[3] G. Y. Tian and A. Sophian, "Defect classification using a new feature for pulsed eddy current sensors," NDT and E International, vol. 38, no. 1, pp. 77-82, 2005.

[4] M. S. Safizadeh, B. A. Lepine, D. S. Forsyth and A. Fahr, "Time-Frequency Analysis of Pulsed Eddy Current Signals," Journal of Nondestructive Evaluation, vol. 20, no. 2, pp. 73-86, 2001.

[5] A. Sophian, Characterisation of Surface and Sub-Surface Discountinuities in Materials Using Pulsed Eddy Current Sensors, PhD Thesis, 2003, pp. 46-51.

[6] F. W. Grover, Inductance Calculations: Working Formulas and Tables (Dover Books on Engineering), Mineola: Dover, 2009.

[7] C. Multiphysiscs, "Comsol Multiphysiscs User's Guide," 2010.

[8] O. C. Zienkiewicz, C. Emson and P. Bettess, "A Novel Boundary Infinite Element," International Journal of Numerical and Methods in Engineering, pp. 393-404, 1983.

[9] J.Jin, The Finite Element Method in Electromagnetics, New York: John Wiley &Sons, 1993.

[10] R.Verfurth, "A Posteriori Error Estimation and Adaptive Mesh-Refinement," Journal of Computational and Applied Mathematics, no. 50, pp. 67-83, 1994.

[11] A. Sophian, G. Y. Tian, D. Taylor and J. Rudlin, "A feature extraction technique based on principal component analysis," NDT and E International, no. 37, pp. 37-41, 2003.

[12] S. Nicola, V. carreto, R. A. mentzer and M. S. Manan, "Corrosion under insulation detection technique," in NACE, Orlando, 2013.

[13] Y. Fu, X. Kang and X. Yu, "Detection of localized corrosion in ferromagnetic metal pipe under insulation with pulsed eddy current testing," Journal of Basic Science and Engineering, vol. 21, no. 4, pp. 786-795, August 2013.